Technology and Economics of Smart Grids and Sustainable Energy (2018) 3: 14
https://doi.org/10.1007/s40866-018-0050-0

ORIGINAL PAPER

Two Novel Approaches of NTSMC and ANTSMC Synchronization for Smart Grid Chaotic Systems

Ali Soltani Sharif Abadi[1] · Pooyan Alinaghi Hosseinabadi[2] · Saad Mekhilef[2]

Received: 11 March 2018 / Accepted: 1 October 2018 / Published online: 28 October 2018

Abstract
The presence of uncertainties and external disturbances is one of the unavoidable problems with various practical systems which might be unavailable in real-time. Sliding Mode Control (SMC) is one of the effective robust control methods to deal with these uncertainties and external disturbances. In this paper, two novel controllers are designed by using Nonsingular Terminal SMC (NTSMC) and Adaptive Nonsingular Terminal SMC (ANTSMC) methods for synchronization of dual smart grid chaotic systems with various uncertainties and external disturbances. Indeed, both adaptive and non-adaptive controllers based on NTSMC are proposed to provide two alternatives which can adjust by changing operating conditions and dynamics. The concept of SMC method guarantees controller robustness against various uncertainties and external disturbances. Elimination of the undesirable chattering phenomenon is addressed in this study which is one of the common deficiencies with conventional SMC method. Additionally, finite time concept is used to speed up the convergence rate. Finite time stability proof is performed by using Lyapunov stability theory. The numerical simulation is carried out in Simulink/MATLAB to reveal the validity of the proposed controllers for the smart grid chaotic system. A comprehensive comparison is made by performing simulation for the Fractional Order Adaptive Sliding Mode Control (FOASMC) controller and defining three performance criteria, among the proposed controllers in this study and FOASMC controller.

Keywords ANTSMC · NTSMC · Synchronization · Control · Smart grid

Introduction

The traditional power systems are based on centralized generation with their large power plants located far from the power consuming loads [21]. Hence the control and centralized operation of this large-scale system is very challenging and complicated task. Smart grids provide smarter operation of conventional power grids by interconnecting the grids in a distributed and interactive manner for the well suitability of distributed multi-agent technologies to alleviate these challenges [24, 25]. Indeed, a smart grids is an electricity network which insists on various operational and energy measures including smart appliances, smart meters, renewable energy resources, and energy efficient resources. Smart grids improve efficiency, minimize cost and consumption of energy, and enhance the reliability and transparency of the energy supply by having a proper control, monitoring, communication and analysis within the supply chain [10, 12, 30].

Recently, many efforts have been made to control these networks. In [24], a multi-agent based protection framework has been proposed to improve the transient stability of smart grids. In [17], a comprehensive review on the control and communication techniques has been done for the smart grids where the energy efficiency of the smart grids

✉ Ali Soltani Sharif Abadi
a.soltanisharif@stu.yazd.ac.ir

Pooyan Alinaghi Hosseinabadi
pooyanalinaghi@siswa.um.edu.my

Saad Mekhilef
saad@um.edu.my

[1] Department of Electrical Engineering, Faculty of Engineering, Yazd University, Yazd, Iran

[2] Power Electronics and Renewable Energy Research Laboratory (PEARL), Department of Electrical Engineering, Faculty of Engineering, University of Malaya, 50603 Kuala Lumpur, Malaysia

has been focused. In (X. [32]), a novel fault tolerant extended Kalman filter has been proposed for smart grid synchronization. a survey of studying complex network theory has been reported in [7] for modern smart grids. In [6], a Cyber-Physical Power System (CPPS) paradigm has been presented for smart transmission grids control, modeling, and monitoring. In [26], a model predictive control (MPC)-based approach has been proposed for smart grids with multiple electric-vehicle charging stations. In [34], a resonance attacks have been investigated on Load Frequency Control of Smart Grids.

The synchronization refers to the process of precisely matching or coordinating two or more activities, processes, devices, or system in time. The synchronization methods have been used in many applications such as synchronization of robots for collaborative robots [29] and the synchronization of chaotic systems with various goals [33, 35]. In [15], the multiagent cooperative controller has been designed for heterogeneous energy storage devices in smart grids considering their hierarchical control structure with droop controls. The active/reactive power sharing, the frequency/voltage, and the energy of battery energy storage systems (BESSs) have been synchronized by exchanging local information with a few other neighboring BESSs.

Finite time stability is a more comprehensive and recent concept than asymptotic stability. The finite time stability means that the system state variables reach zero at the bounded time. The term "terminal" refers to the concept of finite time stability. Many applications require us to prove the stability in a finite time. Accordingly, various finite time theorems and lemmas have been introduced of which some have been presented in [20, 37]. The finite time stability has been very much considered in the recent literature to speed up the convergence rate and improve the concept of stability [11, 18, 37]. In [2], Finite time concept has been considered to incorporate with optimal robust control for Photovoltaic system using the VSC model in Smart Grid.

SMC method is a well-known control method because of its main feature which is robustness against a variety of uncertainties and external disturbances [3, 9]. In [27], optimal real-time control based on the SMC method has been investigated for discrete-time switched repeated scalar nonlinear systems. This robust control method would guarantee asymptotic stability of the systems. The Terminal SMC (TSMC) method has been presented by incorporating finite time concept and SMC method. The TSMC method accomplishes both robustness against external disturbances and uncertainties and system stability in a finite time. Subsequently, a Nonsingular TSMC (NTSMC) method has been introduced to overcome occurrence singularity as an unwanted problem.

On the other hand, the design of the SMC scheme requires the knowledge of uncertainties and external disturbances bound, which might be unavailable in real time. The adaptive concept provides an effective method to deal with these unknown external disturbances and uncertainties by estimating the upper bound of them [4]. Adaptive NTSMC (ANTSMC) method has been proposed by integration of the concept of adaptive control method and NTSMC method. The ANTSMC offers a robust control method with online parameter estimators to provide the information of the uncertainty upper bound. An ANTSMC method has been proposed in [23] to control an autonomous underwater vehicles (AUVs). In (H. [31]), Steer-by-Wire Equipped Road Vehicle has been controlled by using adaptive control concept within a finite time. A fractional order adaptive sliding mode controllers (FOASMC) has been proposed in [14] for a fractional order smart grid chaotic system.

The conventional SMC method causes the unwanted chattering phenomenon due to applying some discontinuous terms in the control input. This undesirable problem causes some devastating effects on the system actuators such as reducing the useful life of them. It also reduces the control accuracy and causes deleterious sound in the system. Hence, numerous approaches have been proposed to eliminate or reduce this destructive phenomenon. The undesirable chattering phenomenon has been thoroughly eliminated in [1, 8, 16, 22, 36]. In [13], an SMC method has been proposed for nonlinear fractional-order systems which has removed the chattering problem completely.

Motivated by the above consideration, in this paper dual smart grid chaotic systems are synchronized by using the NTSMC and ANTSMC methods. Indeed, the adaptive and no-adaptive control methods have been designed by using two novel control inputs. The finite time stability proof is performed by using some finite time lemmas and theories including Barbalet's Lemmas and Lyapunov stability theory. The numerical simulation results of the proposed controllers based on NTSMC and ANTSMC reveal the effectiveness of them to synchronize dual smart grid chaotic system and to suppress the chaotic oscillations. To make a comprehensive comparison, three well-known performance criteria are used including integral of the absolute value of the error (IAE), integral of the time multiplied by the absolute value of the error (ITAE), and integral of the square value (ISV) of the control input. Furthermore, the numerical simulation of the FOASMC is done by applying the control input presented in [14] to the proposed smart grid chaotic system. Note that the numerical simulation of FOASMC has been done to calculate the numerical values of the performance criteria and to show the effectiveness of our proposed controllers compared to the FOASMC controller. The major contributions of the proposed controller designs are listed as follows

- Synchronization of dual smart grid chaotic systems by using two novel adaptive and non-adaptive control methods.
- Elimination of undesirable chattering phenomenon.
- Robust control with the goal of synchronization of two identical chaotic smart grid systems in presence of various uncertainties and external disturbances.
- Estimation of the upper bound of the uncertainties and external disturbances and using their estimations in the control input in the adaptive controllers.
- Guarantee the global finite time stability for all proposed controllers in this study.
- Provide a numerical comparison among the proposed controllers in this study and the FOASMC controller by using three well-known performance criteria, IAE, ITAE, and ISV.

The remaining of this note is organized in the following manner. Section "Mathematical Preliminaries" presents the mathematical preliminaries about the finite time stability theorems and the related lemmas. Section "Model Description of Chaotic Smart Grid and Problem Statement" is dedicated to the model description of the smart grid chaotic system and problem statement. In section "Controller Design", the adaptive and non-adaptive controllers based-on NTSMC are proposed for the smart grid chaotic system along with an explanation of detailed methodology. In section "Results and Discussion", numerical simulation results of proposed controllers are firstly given. Then, comparison and discussion are provided by using three performance criteria. Section "Conclusion" is devoted to the conclusion.

Mathematical Preliminaries

Definition 1: the function of $sgn(x)$ is defined as (2) and the mathematical equality of $sig^{a}(x) = |x|^{a}\, sgn\,(x)$ is always true.

$$sgn(x) = \begin{cases} 1; x > 0 \\ 0; x = 0 \\ -1; x < 0 \end{cases} \tag{1}$$

Lemma 1: consider the nonlinear system as $\dot{x} = f(x), f(0) = 0, x \epsilon \Re^{n}$ with initial conditions $x(0) = x_0$. Suppose there exists candidate Lyapunov function $V(x)$ which is globally positive definite, radially unbounded and only at x = 0 is zero, such that; the time derivative of the candidate Lyapunov function will be as $\dot{V}(x) \leq -\rho_1 V^{\rho_2}(x)$, where ρ_1 is a positive number and ρ_2 is a constant between zero and one. Then, the variable x of the system from any initial conditions, it reaches zero in a finite time, and since then it remains exactly equal to zero, i.e. $\lim_{t \to T} x \to 0$ and the upper bound of the settling time, T, will be as $T \leq \frac{V^{1-\rho_2}(x_0)}{\rho_1(1-\rho_2)}$ [23].

Lemma 2: Assume that $a_1, a_2, \ldots, a_n \Re$ and $0 < q < 2$, then we have [5].

$$|a_1|^{q} + |a_2|^{q} + \ldots + |a_n|^{q} \geq \left(a_1^2 + a_2^2 + \ldots + + a_n^2\right)^{\frac{q}{2}} \tag{2}$$

Lemma 1: Consider the nonlinear system $\dot{x} = f(x) + g(x)u + d$, where d is the model of the uncertainties and external disturbances of the system which is estimated at any moment of time as $h \leq \hat{h}$. At any moment of time, there exist positive constants h^{*}, such that $\hat{h} \leq h^{*}$ [23].

Model Description of Chaotic Smart Grid and Problem Statement

In [14, 28], a model for the smart grid chaotic system has been presented as Eq. (3). Where the vector $X = [x_1, x_2, x_3, x_4]^{T} = [\delta_t, \omega, \delta_L, V_L]^{T}$ is assumed as the vector of system variables. δ_t is the rotator angle and ω is the angular rotation. δ_L is the load voltage angle and V_L is the load voltage. i_o is the inverter current and we have $s(\vartheta) = \sin(\vartheta)$, $c(\vartheta) = \cos(\vartheta)$.

$$\begin{cases} \dot{x}_1 = x_2 \\ \dot{x}_2 = 0.573 - 0.167x_2 + 20x_4 c(x_1 - x_3 + 1.483) \\ \quad + 11.667x_4 c(x_1 + 1.483) \\ \dot{x}_3 = 69 - 93.33x_4 - 179.05x_4^2 - 50i_o x_4 s(x_3) \\ \quad - 300x_4 s(x_3) c(x_1 - 1.483) \\ \dot{x}_4 = 25.322x_4^2 + 13.054x_4 + 3.529x_4 c(x_1 - 1.483) \\ 3.529x_4 c(x_3) c(x_3 - 1.483) - 42.353x_4 s(x_3 + 1.483) \\ -35.294x_4 s(x_3 + 1.483) + 2.941x_4 c(x_3 - 1.483) \\ +42.353x_4 s(x_3) c(x_1 - 1.483) + 7.059i_o x_4 s(x_3) \\ +0.588i_o x_4 c(x_3) + 1.31778 \end{cases} \tag{3}$$

Where this system shows chaotic behavior for the $i_o = 0.01$ and selected initial conditions as $X(0) = [0.3, 0.2, 0.1, 0.97]^{T}$. Figures 1, 2 and 3 display the 3D-phase diagram of the chaotic behavior of the smart grid system.

In this paper, we intend to synchronize two identical chaotic systems presented in Eq. (3). For this purpose, the master system is considered as Eq. (4) and the slave system is considered as Eq. (6).

$$\begin{cases} \dot{x}_{1_m} = f_{1_m} + d_{1_m} \\ \dot{x}_{2_m} = f_{2_m} + d_{2_m} \\ \dot{x}_{3_m} = f_{3_m} + d_{3_m} \\ \dot{x}_{4_m} = f_{4_m} + d_{4_m} \end{cases} \tag{4}$$

Where $d_{i_m}, i = (1, 2, 3, 4)$ is a variety of uncertainties and external disturbances. Note that, f_{i_m} is presented in Eq. (5).

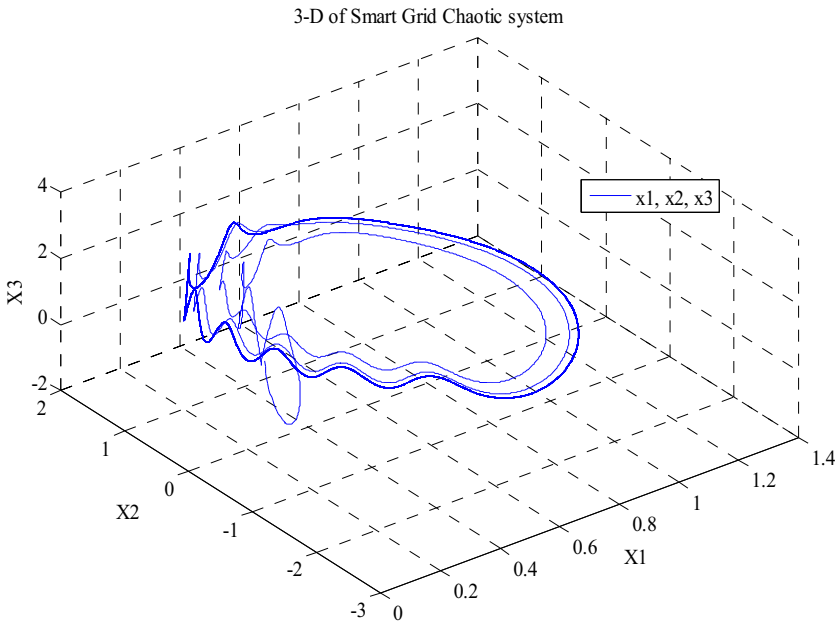

Fig. 1 3D-phase diagram of variables x_1, x_2, x_3 of the smart grid system

$$
\begin{cases}
f_{1_m} = x_{2_m} \\
f_{2_m} = 0.573 - 0.167 x_{2_m} \\
\quad +20 x_{4_m} c(x_{1_m} - x_{3_m} + 1.483) \\
\quad +11.667 x_{4_m} c(x_{1_m} + 1.483) \\
f_{3_m} = 69 - 93.33 x_{4_m} - 179.05 x_{4_m}^2 - 50 i_o x_{4_m} s(x_{3_m}) \\
\quad -300 x_{4_m} s(x_{3_m}) c(x_{1_m} - 1.483) \\
f_{4_m} = 25.322 x_{4_m}^2 + 13.054 x_{4_m} \\
\quad +3.529 x_{4_m} c(x_{1_m} - 1.483) \\
\quad -3.529 x_{4_m} c(x_{3_m}) c(x_{3_m} - 1.483) \\
\quad +42.353 x_{4_m} s(x_{3_m}) c(x_{1_m} - 1.483) \\
+7.059 i_o x_{4_m} s(x_{3_m}) - 42.353 x_{4_m} s(x_{3_m} + 1.483) \\
-35.294 x_{4_m} s(x_{3_m} + 1.483) + 0.588 i_o x_{4_m} c(x_{3_m}) \\
\quad +2.941 x_{4_m} c(x_{3_m} - 1.483) + 1.31778
\end{cases} \tag{5}
$$

The slave system is as follows

$$
\begin{cases}
\dot{x}_{1_s} = f_{1_s} + u_1 + d_{1_s} \\
\dot{x}_{2_s} = f_{2_s} + u_2 + d_{2_s} \\
\dot{x}_{3_s} = f_{3_s} + u_3 + d_{3_s} \\
\dot{x}_{4_s} = f_{4_s} + u_4 + d_{4_s}
\end{cases} \tag{6}
$$

Where $d_{i_s}, i = (1, 2, 3, 4)$ is a variety of uncertainties and external disturbances. u_i is the control input that will be designed. Note that, f_{i_s} is presented in Eq. (7).

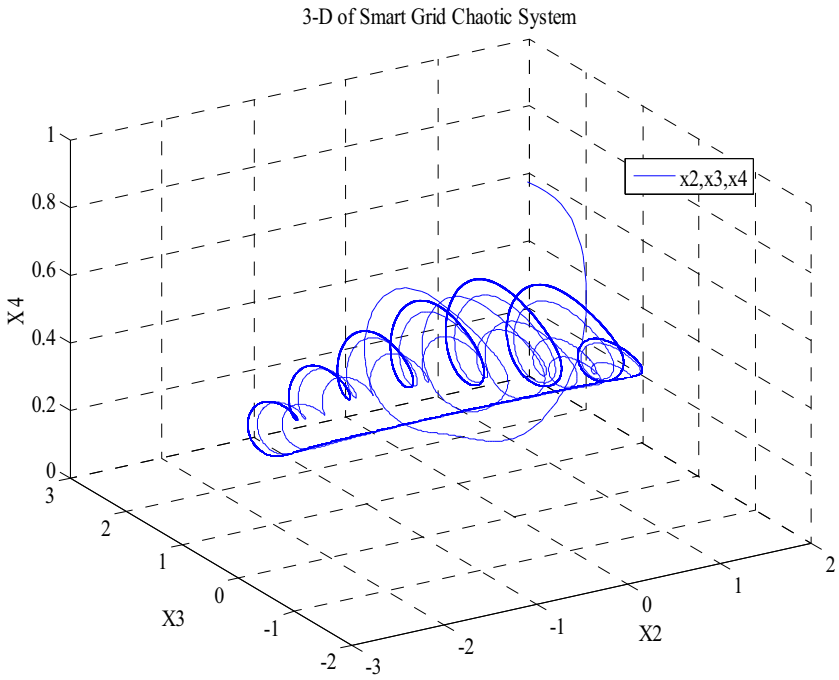

Fig. 2 3D-phase diagram of variables x_2, x_3, x_4 of the smart grid system

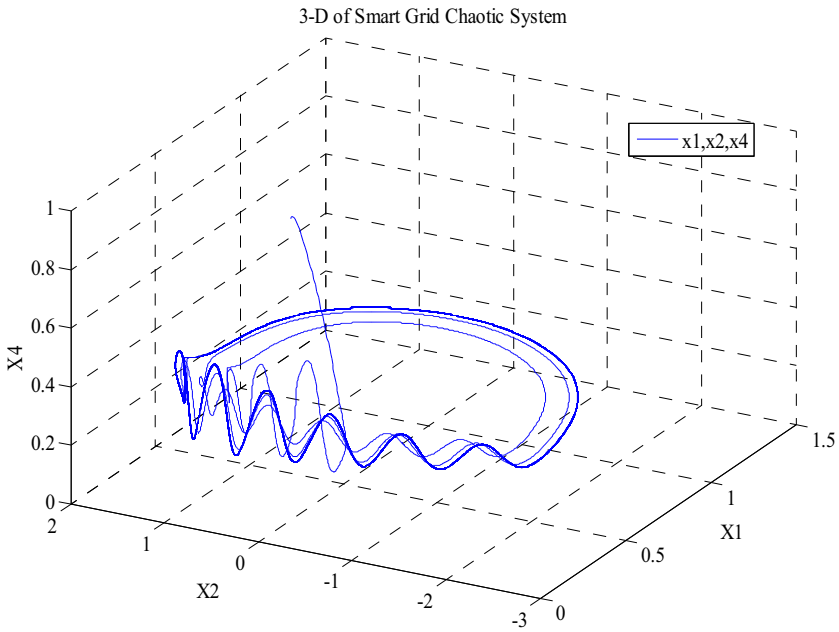

Fig. 3 3D-phase diagram of variables x_1, x_2, x_4 of the smart grid system

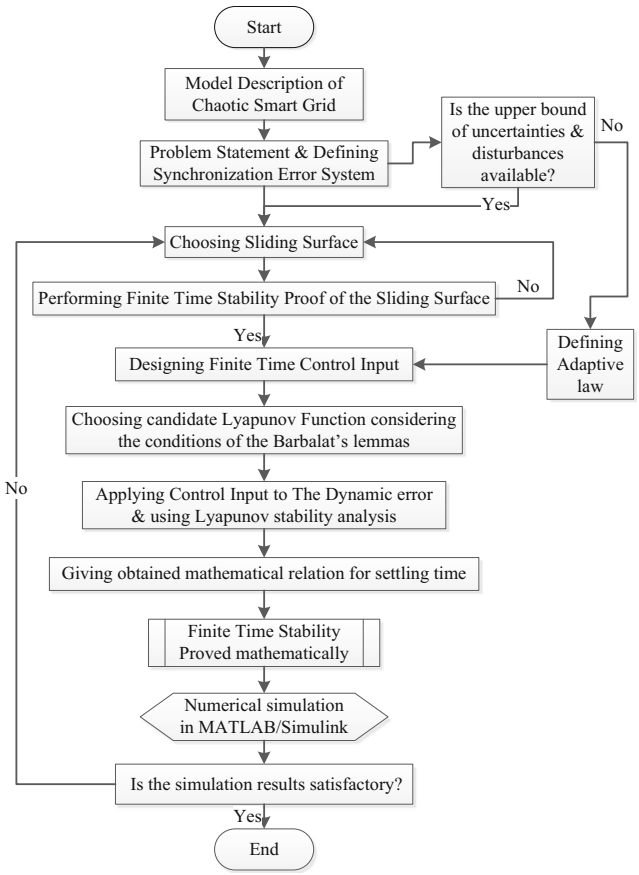

Fig. 4 3Flow chart of the methodology for the proposed controller designs

$$
\begin{cases}
f_{1_s} = x_{2_s} \\
f_{2_s} = 0.573 - 0.167x_{2_s} \\
\quad +20x_{4_s}c(x_{1_s} - x_{3_s} + 1.483) \\
\quad +11.667x_{4_s}c(x_{1_s} + 1.483) \\
f_{3_s} = 69 - 93.33x_{4_s} - 179.05x_{4_s}^2 - 50i_o x_{4_s}s(x_{3_s}) \\
\quad -300x_{4_s}s(x_{3_s})c(x_{1_s} - 1.483) \\
f_{4_s} = 25.322x_{4_s}^2 + 13.054x_{4_s} \\
\quad +3.529x_{4_s}c(x_{1_s} - 1.483) \\
\quad -3.529x_{4_s}c(x_{3_s})c(x_{3_s} - 1.483) \\
\quad +42.353x_{4_s}s(x_{3_s})c(x_{1_s} - 1.483) \\
+7.059i_o x_{4_s}s(x_{3_s}) - 42.353x_{4_s}s(x_{3_s} + 1.483) \\
-35.294x_{4_s}s(x_{3_s} + 1.483) + 0.588i_o x_{4_s}c(x_{3_s}) \\
\quad +2.941x_{4_s}c(x_{3_s} - 1.483) + 1.31778
\end{cases} \tag{7}
$$

For the synchronization of two identical chaotic systems (mater and slave systems), the synchronization error system will be defined as $e_i = x_{i_s} - x_{i_m}$. Hence, the synchronization error system is given as Eq. (8)

$$
\begin{cases}
\dot{e}_1 = f_{1_s} - f_{1_m} + u_1 + d_1 \\
\dot{e}_2 = f_{2_s} - f_{2_m} + u_2 + d_2 \\
\dot{e}_3 = f_{3_s} - f_{3_m} + u_3 + d_3 \\
\dot{e}_4 = f_{4_s} - f_{4_m} + u_4 + d_4
\end{cases} \tag{8}
$$

Where we have $d_i = d_{i_s} - d_{i_m}$. In the following sections, control inputs, u_i are designed; in such a way that, by applying these designed control inputs, the system will be stable in a finite time and robust against various uncertainties and external disturbances.

Controller Design

In order to achieve the proposed controllers in this study, some mathematical finite-time theorem and lemmas are used such as the Lyapunov stability theory and Barbalat's lemmas. First, the chaotic dynamics of the smart grid is presented in presence of the uncertainties and external disturbances. Then, the finite time stability proofs are performed mathematically by applying the designed controllers into the proposed system. Then the numerical simulation results are carried out in MATLAB/Simulink to verify the validity of proposed controller designs and comparing them. Note that the non-adaptive control methods (NTSMC) are designed by assuming that the upper bound of uncertainties and external disturbances is available. On the contrary, the adaptive control methods (ANTSMC) are designed by assuming that the upper bound of uncertainties and external disturbances is not available and needs to estimate. For this reason, the adaptive concept is employed to deal with these unknown external disturbances and uncertainties by estimating the upper bound of them (where their estimations are used in the control input). In fact, both adaptive and non-adaptive controllers based on NTSMC are proposed to provide two alternatives which can adjust by changing operating conditions and dynamics and comparing them from various aspects. The flow chart of the methodology for the proposed controllers with detail mathematic procedures represents in Fig. 4.

Two Novel Approaches of Terminal Sliding Mode Control

In this section, two control inputs are designed by using two different sliding surfaces based on the NTSMC method (non-adaptive control methods) for the presented synchronization error system of Eq. (8). Note that the upper bound of the sum of the uncertainties and external disturbances (d_i) and their derivatives ($\dot{d}_i$) are assumed to be available; accordingly, we have

$$\begin{cases} ||d_i|| \le \eta_{i_1} \\ ||\dot{d}_i|| \le \eta_{i_2} \end{cases} \tag{9}$$

Theorem1 (NTSMC1) By considering a system in Eq. (8), and the considered conditions for the upper bound of the uncertainties and external disturbances in Eq. (9), using the sliding surfaces in Eq. (10), and the designed control input in Eq. (11), the finite time stability will be guaranteed. Therefore, the slave system will be synchronized to the master system in the finite time T. Note that the stability time for the system is the sum of the stability of sliding surfaces (T_r) and the reaching time to the sliding surfaces (T_s). Accordingly, the stability time of the system is equal to $T = T_r + T_s$, of which the upper bound of T_r, T_s is presented in the following.

$$\begin{cases} s_1 = \int_0^{t_f} e_1 d_t + \alpha_{11} e_1^{\alpha_{21}} \\ s_2 = \int_0^{t_f} e_2 d_t + \alpha_{12} e_2^{\alpha_{22}} \\ s_3 = \int_0^{t_f} e_3 d_t + \alpha_{13} e_3^{\alpha_{23}} \\ s_4 = \int_0^{t_f} e_4 d_t + \alpha_{14} e_4^{\alpha_{24}} \end{cases} \tag{10}$$

Where α_{1i} are positive constants and α_{2i} are constants between one and zero.

$$\begin{cases} u_i = u_{eq_i} + u_{r_i} \\ u_{eq_i} = -(f_{i_s} - f_{i_m}) - \alpha_{1i}^{-1} \alpha_{2i}^{-1} e_1^{-\alpha_{2i}^{-1}+2} \\ u_{r_i} = -c_{1i} sig^{\beta_{1i}}(s_i) - \eta_{i_1} sgn(s_i) \end{cases} \tag{11}$$

Where c_{1i} are positive constants and β_{1i} are constants between one and zero.

Proof To prove the finite time stability of the system in Eq. (8), we need firstly to prove that the system reaches to the sliding surface in a finite time by using the designed control input in Eq. (11). Hence, the candidate Lyapunov function is considered as $V(x) = \sum_{i=1}^{4} \frac{1}{2} s_i^2$. This candidate function possesses condition of Lyapunov function in lemma 1. By differentiating this candidate function with respect to time and applying the control input to the system, yields

$$\dot{V}(x) = \sum_{i=1}^{4} s_i \left(-c_{1i} sig^{\beta_{1i}}(s_i) - \eta_{i_1} sgn(s_i) + d_i \right) \tag{12}$$

Since we have $\|d_i\| \le \eta_{i_1}$ and in accordance with definition 1, there comes

$$\dot{V}(x) \le -\sum_{i=1}^{4} c_{1i} |s_i|^{\beta_{1i}+1} \tag{13}$$

By substituting $|s_i| = \sqrt{2}\sqrt{V(x)}$ into Eq. (13) and in accordance with lemma 2, one can obtain

$$\dot{V}(x) \le -\sum_{i=1}^{4} c_{1i} \left(\sqrt{2}\sqrt{V(x)} \right)^{\beta_{1i}+1} \tag{14}$$

Now, by choosing $\rho_1 = c_{1i} \left(\sqrt{2}\right)^{\beta_{1i}+1}$ and $\rho_2 = \frac{\beta_{1i}+1}{2}$, we have

$$\dot{V}(x) \le -\rho_1 V^{\rho_2} \tag{15}$$

According to Lemma 1, the system reaches to the sliding surfaces in a finite time as $T_s \le 4 \frac{(V(x(0)))^{\rho_2}}{\rho_1 (1-\rho_2)}$.

For the second part of the system stability proof, the finite time stability proof of the sliding surface of $s_i = 0$ must be performed. For this purpose, the Eq. (10) is equalized to zero, and then its time derivation is taken as follows (note that $s_i = \int_0^{t_f} e_i + \alpha_{1i} e_i^{\alpha_{2i}}$ is a general form of Eq. (10))

$$\dot{s}_i = 0 \rightarrow \dot{e}_i = -\alpha_{2i}^{-1} \alpha_{1i}^{-1} e_i^{2-\alpha_{2i}} \tag{16}$$

Also, we have

$$e_i(t) = \left(e^{\alpha_{2i}-1}(t_{si}) - \alpha_{2i-1}^{-1}\left(1-\alpha_{2i}^{-1}\right)(t-t_{si})\right)^{\frac{1}{\alpha_{2i}-1}} \quad (17)$$

The numerical solution of Eq. (17) shows that the variables converge to zero in the finite time, T_r, and the upper bound of this time is as below [23].

$$T_r \leq \sum_{i=1}^{4} \frac{\alpha_{1i}}{\left(1-\alpha_{2i}^{-1}\right)} |e(T_{s_i})|^{(\alpha_{2i}-1)} \quad (18)$$

As a result, the system finite time stability proof is completed and the system stability time is as $T = T_r + T_s$. ∎.

Note that using the *sgn* function in the designed control input in this section is likely to cause the undesirable chattering phenomenon. To overcome this deficiency, we will design control input in the next section in such a way that we use of integral of *sgn* function in the control input, which can reduce or eliminate this unwanted problem.

Theorem 2 (NTSMC2) By considering the system in Eq. (8), and the considered conditions for the upper bound of the uncertainties and external disturbances in Eq. (9), using the sliding surfaces in Eq. (19), and the designed control input in Eq. (20), the finite time stability will be guaranteed. Therefore, the slave system will be synchronized to the master system in the finite time T. Note that the stability time for the system is the sum of the stability of sliding surfaces (T_r) and the reaching time to the sliding surfaces (T_s). Accordingly, the stability time of the system is equal to $T = T_r + T_s$, of which the upper bound of T_r, T_s is presented in the following.

$$\begin{cases} s_1 = \dot{e}_1 + \alpha_{11} e_1^{\alpha_{21}} \\ s_2 = \dot{e}_2 + \alpha_{12} e_2^{\alpha_{22}} \\ s_3 = \dot{e}_3 + \alpha_{13} e_3^{\alpha_{23}} \\ s_4 = \dot{e}_4 + \alpha_{14} e_4^{\alpha_{24}} \end{cases} \quad (19)$$

Where α_{1i} are positive constants and α_{2i} are constants between one and zero.

$$\begin{cases} u_i = u_{eq_i} + u_{r_i} \\ u_{eq_i} = -\left(f_{i_s} - f_{i_m}\right) - \alpha_{1i} e_i^{\alpha_{2i}} \\ \dot{u}_{r_i} = -c_{1i} sig^{\beta_{1i}}(s_i) - \eta_{i_2} sgn(s_i) \end{cases} \quad (20)$$

Where c_{1i} are positive constants and β_{1i} are constants between one and zero.

Proof To prove the finite time stability of the system in Eq. (8), we need firstly to prove that the system reaches to the sliding surface in a finite time by using the designed control input in Eq. (20). Hence, the candidate Lyapunov function is considered as $V(x) = \sum_{i=1}^{4} \frac{1}{2} s_i^2$. This candidate function possesses condition of Lyapunov function in lemma 1. By differentiating this candidate function with respect to time and applying the control input to the system, yields

$$\dot{V}(x) = \sum_{i=1}^{4} s_i \left(-c_{1i} sig^{\beta_{1i}}(s_i) - \eta_{i_2} sgn(s_i) + \dot{d}_i\right) \quad (21)$$

Since we have $\|d_i\| \leq \eta_{i_1}$ and in accordance with definition 1, there comes

$$\dot{V}(x) \leq -\sum_{i=1}^{4} c_{1i} |s_i|^{\beta_{1i}+1} \quad (22)$$

By substituting $|s_i| = \sqrt{2}\sqrt{V(x)}$ into Eq. (22) and in accordance with lemma 2, one can obtain

$$\dot{V}(x) \leq -\sum_{i=1}^{4} c_{1i} \left(\sqrt{2}\sqrt{V(x)}\right)^{\beta_{1i}+1} \quad (23)$$

Now, by choosing $\rho_1 = c_{1i}\left(\sqrt{2}\right)^{\beta_{1i}+1}$ and $\rho_2 = \frac{\beta_{1i}+1}{2}$, we have

$$\dot{V}(x) \leq -\rho_1 V^{\rho_2} \quad (24)$$

According to lemma 1, the system reaches to the sliding surfaces in a finite time as $T_s \leq 4 \frac{(V(x(0)))^{\rho_2}}{\rho_1(1-\rho_2)}$.

For the second part of the system stability proof, the finite time stability proof of the sliding surface of $s_i = 0$ must be performed. For this purpose, the Eq. (19) is equalized to zero, and then its time derivation is taken as follows (note that $s_i = \dot{e}_i + \alpha_{1i} e_i^{\alpha_{2i}}$ is a general form of Eq. (19))

$$\dot{s}_i = 0 \rightarrow \dot{e}_i = -\alpha_{1i} e_i^{\alpha_{2i}} \quad (25)$$

Also, we have

$$e_i(t) = \left(e^{\alpha_{2i}-1}\left(t_{si}\right) - \alpha_{2i-1}^{-1}\left(1-\alpha_{2i}^{-1}\right)(t-t_{si})\right)^{\frac{1}{\alpha_{2i}-1}} \quad (26)$$

The numerical solution of Eq. (26) shows that the variables converge to zero in the finite time, T_r, and the upper bound of this time is as below [23]

$$T_r \leq \sum_{i=1}^{4} \frac{\alpha_{1i}}{\left(1-\alpha_{2i}^{-1}\right)} |e(T_{s_i})|^{(\alpha_{2i}-1)} \quad (27)$$

As a result, the system finite time stability proof is completed and the system stability time is as $T = T_r + T_s$. ∎

Two Novel Approaches of Adaptive Nonsingular Terminal Sliding Mode Control

In this section, two control inputs are designed by using two different sliding surfaces based on the ANTSMC method (adaptive control methods) for the presented synchronization error system of Eq. (8). The adaptive concept is used to estimate the unknown external disturbances and uncertainties and their estimation is used in the both designed control inputs. Note that the upper bound of the sum of the uncertainties and external disturbances (d_i) are assumed to be not available and need to estimate, accordingly we have (in accordance with lemma 3)

$$d_i = h_i|p_i(x)| \le \hat{h}_i|p_i(x)| \le h_i^*|p_i(x)| \tag{28}$$

Where $\hat{h}$ is the estimation of the unknown upper bound of the uncertainties and external disturbances. h^* is the upper bound of this estimation which exists according to Lemma 3. Also, $|p(x)|$ is a nonlinear function of the model of uncertainties and external disturbances.

Theorem 3 (ANTSMC1) By considering the system in Eq. (8), and the considered conditions for the upper bound of the uncertainties and external disturbances in Eq. (28), using the sliding surfaces in Eq. (10), which is repeated in (29), and the designed control input in Eq. (30), as well as the adaptive laws in relation (31), the finite time stability will be guaranteed. Therefore, the slave system will be synchronized to the master system in the finite time T. Note that the stability time for the system is the sum of the stability of sliding surfaces (T_r) and the reaching time to the sliding surfaces (T_s). Accordingly, the stability time of the system is equal to $T = T_r + T_s$, of which the upper bound of T_r, T_s is presented in the following. Note that the unknown upper bound of uncertainties and external disturbances are estimated in this finite time T and their estimation used in the control input.

$$\begin{cases} s_1 = \int_0^{t_f} e_1 d_t + \alpha_{11} e_1^{\alpha_{21}} \\ s_2 = \int_0^{t_f} e_2 d_t + \alpha_{12} e_2^{\alpha_{22}} \\ s_3 = \int_0^{t_f} e_3 d_t + \alpha_{13} e_3^{\alpha_{23}} \\ s_4 = \int_0^{t_f} e_4 d_t + \alpha_{14} e_4^{\alpha_{24}} \end{cases} \tag{29}$$

Where α_{1i} are positive constants and α_{2i} are constants between one and zero.

$$\begin{cases} u_i = u_{eq_i} + u_{r_i} \\ u_{eq_i} = -\left(f_{i_s} - f_{i_m}\right) - \alpha_{1i}^{-1}\alpha_{2i}^{-1} e_1^{-\alpha_{2i}^{-1}+2} \\ u_{r_i} = -\hat{h}_i sgn(s_i)|p_i(x)| \end{cases} \tag{30}$$

Where c_{1i} are positive constants and β_{1i} are constants between one and zero.

$$\dot{\hat{h}}_i = \delta_i \alpha_{1i}\alpha_{2i} e_i^{\alpha_{2i}-1}|s_i||p_i(x)| \tag{31}$$

Where δ_i are positive constants and less than one.

Proof 3 To prove the finite time stability of the system in Eq. (8), we need firstly to prove that the system reaches to the sliding surface in a finite time by using the designed control input in Eq. (30). Hence, the candidate Lyapunov function is considered as $V(x) = \sum_{i=1}^{4} \frac{1}{2} s_i^2 + \frac{1}{2}\tilde{h}_i^2$, where we have $\tilde{h}_i = \hat{h}_i - h_i^*$. This candidate function possesses condition of Lyapunov function in lemma 1. By differentiating this candidate function with respect to time and by considering $\dot{\tilde{h}}_i = \dot{\hat{h}}_i$, yields

$$\dot{V}(x) = \sum_{i=1}^{4} s_i \dot{s}_i + \dot{\hat{h}}_i \tilde{h}_i \tag{32}$$

By differentiating the Eq. (29) with respect to time and applying the control input (30), resulting in

$$\begin{aligned} \dot{V}(x) = \sum_{i=1}^{4} s_i \alpha_{1i}\alpha_{2i} e_i^{\alpha_{2i}-1} \left(-\hat{h}_i sgn(s_i)|p_i(x)| + h_i|p_i(x)|\right) \\ + \left(\delta_i \alpha_{1i}\alpha_{2i} e_i^{\alpha_{2i}-1}|s_i||p_i(x)|\right)\tilde{h}_i \end{aligned} \tag{33}$$

By adding the term $\pm\sum_{i=1}^{4} \alpha_{1i}\alpha_{2i} e_i^{\alpha_{2i}-1}|s_i|h_i^*$ to Eq. (33), yields

$$\begin{aligned} \dot{V}(x) \le \sum_{i=1}^{4} -|s_i|\left(\alpha_{1i}\alpha_{2i} e_i^{\alpha_{2i}-1}\left(h_i^*|p_i(x)| - h_i|p_i(x)|\right)\right) \\ -\left(\alpha_{1i}\alpha_{2i} e_i^{\alpha_{2i}-1}|s_i||p_i(x)|\right)(1-\delta_i)|\tilde{h}_i| \end{aligned} \tag{34}$$

By assuming $\Delta_1 = \sum_{i=1}^{4}\left(\alpha_{1i}\alpha_{2i} e_i^{\alpha_{2i}-1}\left(h_i^*|p_i(x)| - h_i|p_i(x)|\right)\right)$ and $\Delta_2 = \sum_{i=1}^{4} \alpha_{1i}\alpha_{2i} e_i^{\alpha_{2i}-1}|s_i|\ |p_i(x)|\ (1-\delta_i)$, there comes

$$\dot{V}(x) \le \sum_{i=1}^{4} -|s_i|(\Delta_1) - (\Delta_2)|\tilde{h}_i| \tag{35}$$

Then, by defining Δ_{min} as $\Delta_{min} = \min\left(\sqrt{2}\Delta_1, \sqrt{2}\Delta_2\right)$ and in accordance with lemma 2, we have

$$\dot{V}(x) \le -\Delta_{min} V^{\frac{1}{2}}(x) \tag{36}$$

Finally, by choosing $\rho_1 = \Delta_{min}$ and $\rho_2 = \frac{1}{2}$, yields

$$\dot{V}(x) \le -\rho_1 V^{\rho_2}(x) \tag{37}$$

According to Lemma 1, the system reaches to the sliding surfaces in a finite time as $T_s \le 4\frac{(V(x(0)))^{\rho_2}}{\rho_1\left(\frac{1}{2}\right)}$.

The second part of the system stability proof is investigating the finite time stability of the sliding surface in Eq. (10) (which is repeated in Eq. (29)). In Eqs. (16) and (17) the finite time stability proof of the sliding surfaces of Eq. (29) or Eq. (10) has been performed. Also, its stability time has been presented in Eq. (18).

As a result, the system finite time stability proof is completed and the system stability time is as $T = T_r + T_s$. ∎

Theorem 4 (ANTSMC2) By considering the system in Eq. (8), and the considered conditions for the upper bound of the uncertainties and external disturbances in Eq. (28), using the sliding surfaces in Eq. (19), which is repeated in (37), and the designed control input in Eq. (38), as well as the adaptive laws in relation (39), the finite time stability will be guaranteed. Therefore, the slave system will be synchronized to the master system in the finite time T. Note that the stability time for the system is the sum of the stability of sliding surfaces (T_r) and the reaching time to the sliding surfaces (T_s).

Accordingly, the stability time of the system is equal to $T = T_r + T_s$, of which the upper bound of T_r, T_s is presented in the following. Note that the unknown upper bound of uncertainties and external disturbances are estimated in this finite time T and their estimation used in the control input.

$$\begin{cases} s_1 = \dot{e}_1 + \alpha_{11} e_1^{\alpha_{21}} \\ s_2 = \dot{e}_2 + \alpha_{12} e_2^{\alpha_{22}} \\ s_3 = \dot{e}_3 + \alpha_{13} e_3^{\alpha_{23}} \\ s_4 = \dot{e}_4 + \alpha_{14} e_4^{\alpha_{24}} \end{cases} \tag{38}$$

Where α_{1i} are positive constants and α_{2i} are constants between one and zero.

$$\begin{cases} u_i = u_{eq_i} + u_{r_i} \\ u_{eq_i} = -\left(f_{i_s} - f_{i_m}\right) - \alpha_{1i} e_i^{\alpha_{2i}} \\ u_{r_i} = -\hat{h}_i sgn(s_i)|p_i(x)| \end{cases} \tag{39}$$

Where c_{1i} are positive constants and β_{1i} are constants between one and zero.

$$\dot{\hat{h}}_i = \delta_i |s_i||p_i(x)| \tag{40}$$

Where δ_i are positive constants and less than one.

Proof 4 To prove the finite time stability of the system in Eq. (8), we need first to prove that the system reaches to the sliding surface in a finite time by using the designed control input in Eq. (39). Hence, the candidate Lyapunov function is considered as $V(x) = \sum_{i=1}^{4} \frac{1}{2} s_i^2 + \frac{1}{2} \tilde{h}_i^2$, where we have $\tilde{h}_i = \hat{h}_i - h_i^*$. This candidate function possesses condition of Lyapunov function in lemma 1. By differentiating this candidate function with respect to time and by considering $\dot{\tilde{h}}_i = \dot{\hat{h}}_i$, yields

$$\dot{V}(x) = \sum_{i=1}^{4} s_i \dot{s}_i + \dot{\hat{h}}_i \tilde{h}_i \tag{41}$$

By differentiating the Eq. (38) with respect to time and applying the control input (39), resulting in

$$\dot{V}(x) = \sum_{i=1}^{4} \begin{matrix} s_i \left(-\hat{h}_i |p_i(x)| + h_i |p_i(x)| \right) \\ + (-2|s_i||p_i(x)|) \tilde{h}_i \end{matrix} \tag{42}$$

By adding the term $\pm \sum_{i=1}^{4} |s_i| h_i^*$ to Eq. (42), yields

$$\dot{V}(x) \le \sum_{i=1}^{4} -|s_i| \left(\left(h_i^* |p_i(x)| - h_i |p_i(x)| \right) \right) - (|s_i||p_i(x)|) |\tilde{h}_i| \tag{43}$$

By assuming $\Delta_1 = \sum_{i=1}^{4} \left(\left(h_i^* |p_i(x)| - h_i |p_i(x)| \right) \right)$ and $\Delta_2 = \sum_{i=1}^{4} |s_i| \, |p_i(x)| \, (1 - \delta_i)$, there comes

$$\dot{V}(x) \le \sum_{i=1}^{4} -|s_i| (\Delta_1) - (\Delta_2) |\tilde{h}_i| \tag{44}$$

Then, by defining Δ_{min} as $\Delta_{min} = \min\left(\sqrt{2}\Delta_1, \sqrt{2}\Delta_2 \right)$ and in accordance with lemma 2, we have

$$\dot{V}(x) \le -\Delta_{min} V^{\frac{1}{2}}(x) \tag{45}$$

Finally, by choosing $\rho_1 = \Delta_{min}$ and $\rho_2 = \frac{1}{2}$, yields

$$\dot{V}(x) \le -\rho_1 V^{\rho_2}(x) \tag{46}$$

According to Lemma 1, the system reaches to the sliding surfaces in a finite time as $T_s \le 4 \frac{(V(x(0)))^{\rho_2}}{\rho_1 \left(\frac{1}{2} \right)}$.

The second part of the system stability proof is investigating the finite time stability of the sliding surface in Eq. (19) (which is repeated in Eq. (37)). In Eqs. (25) and (26) the finite time stability proof of the sliding surfaces of Eq. (37) or Eq. (19) has been performed. Also, its stability time has been presented in Eq. (27).

As a result, the system finite time stability proof is completed and the system stability time is as $T = T_r + T_s$. ∎

Results and Discussion

Numerical Simulation

In this section, the numerical simulations of the four proposed control approaches have been done for the smart grid chaotic system. The numerical simulation results are carried out in Simulink/MATLAB by using the ode45 solver and with a simulation step size of 0.001. The initial conditions of the master system have been considered as in Section "Model Description of Chaotic Smart Grid and Problem Statement". All initial conditions of the slave systems have been considered zero, i.e. $X_s(0) = [0, 0, 0, 0]^T$. The selected control parameters for this simulation are presented in Table 1.

Also, we have

$$\begin{matrix} c_{1i} = 0.5, |p_i(x)| = |x_{i_s} - x_{i_m}|, \\ d_i = |x_{i_s} - x_{i_m}|, \delta_i = 0.5 \end{matrix} \tag{47}$$

The upper bound of the uncertainties and external disturbances is considered for two non-adaptive approaches of NTSMC, as a constant and equal to one i.e.

Table 1 Selected control parameters for the proposed controllers

	NTSMC1	NTSMC2	ANTSMC1	ANTSMC2
α_{11}	5.99	60	0.03	60
α_{12}	0.04	60	0.03	60
α_{13}	0.04	60	0.03	60
α_{14}	0.04	60	0.03	60
α_{21}	103/101	7/5	7/5	7/5
α_{22}	103/101	7/5	7/5	7/5
α_{23}	103/101	7/5	7/5	7/5
α_{24}	103/101	7/5	7/5	7/5

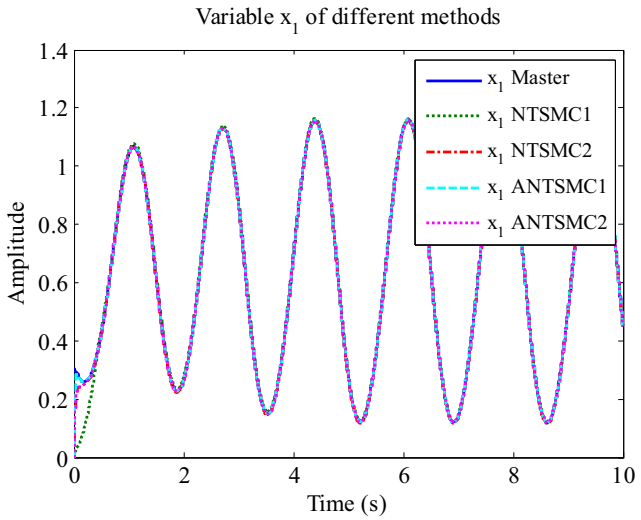

Fig. 5 The state variable x_1 of four proposed control methods

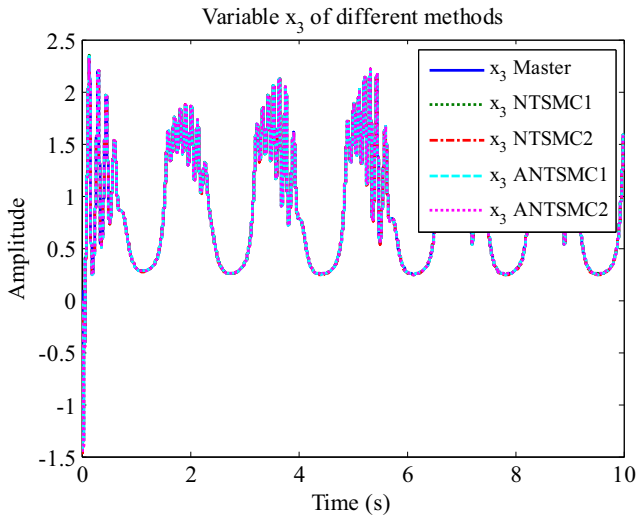

Fig. 7 The state variable x_3 of four proposed control methods

$\eta_{i_1} = 1, \eta_{i_2} = 100$. Figures 5, 6, 7 and 8, represent the state variables x_1 to x_4 of the master and slave systems for four designed control methods. It can be obviously observed that the state variables of the slave system (by applying the proposed controllers) converge precisely to the state variables of the master system in a finite time (approximately in less than 1 s). In other words, the synchronization errors converge to zero precisely as soon as the controller is introduced (see Figs. 5 to 8).

Figures 9, 10, 11 and 12 show the control inputs u_1 to u_4 for four designed control methods. The unwanted chattering phenomenon is observed (see Fig. 9) in the control input of the first designed non-adaptive control method (NTSMC1). However, this undesirable phenomenon is eliminated completely in the designed control inputs of the proposed NTSMC2, ANTSMC1, and ANTSMC2 (see Figs. 9 to 12).

Comparison and Discussion

To perform a comprehensive comparison, the three following performance criteria, IAE, ITAE, and ISV are used which have been presented in [19]. Note that, if the numerical value of each performance criterion is less than another one, it will signify that the method is more appropriate. The performance criteria are defined as follows

(a) Integral of the absolute value of the error (IAE)

$$IAEi = \int_0^{t_f} |e_i(t)| dt \tag{48}$$

(b) Integral of the time multiplied by the absolute value of the error (ITAE)

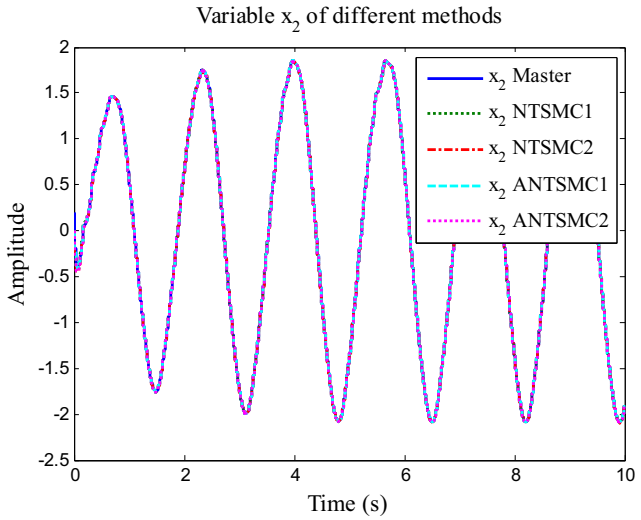

Fig. 6 The state variable x_2 of four proposed control methods

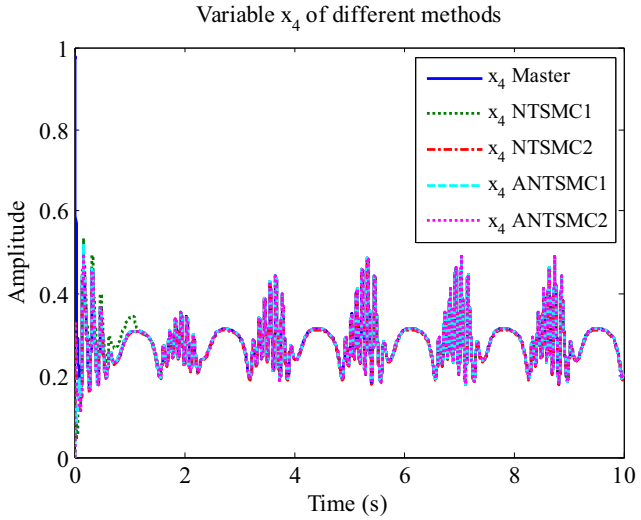

Fig. 8 The state variable x_4 of four proposed control methods

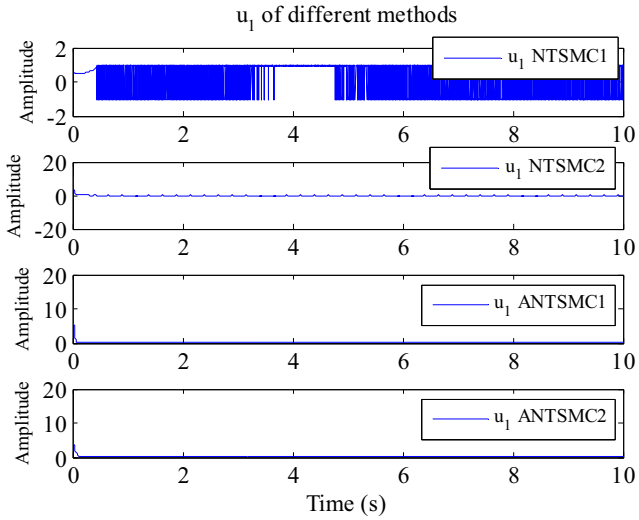

Fig. 9 The control inputs $\boldsymbol{u_1}$ of four proposed control methods

$$ITAEi = \int_0^{t_f} t|e_i(t)|dt \tag{49}$$

(c) Integral of the square value (ISV) of the control input

$$ISVi = \int_0^{t_f} |u_i(t)|^2 dt \tag{50}$$

The IAE and ITAE are used as the goal numerical measures of tracking performance for an entire error curve, where t_f shows the total running time. The IAE criterion will provide an intermediate result. In the ITAE criterion, time appears as a factor, which will deeply emphasize the errors that occur late in time. The ISV criterion represents the consumption of energy [19].

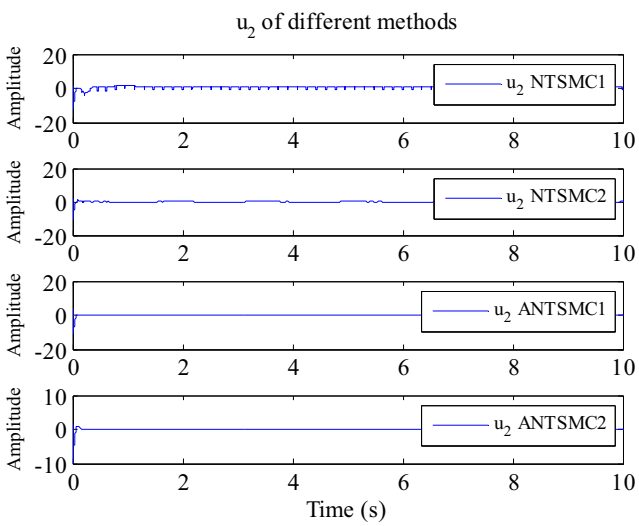

Fig. 10 The control inputs $\boldsymbol{u_2}$ of four proposed control methods

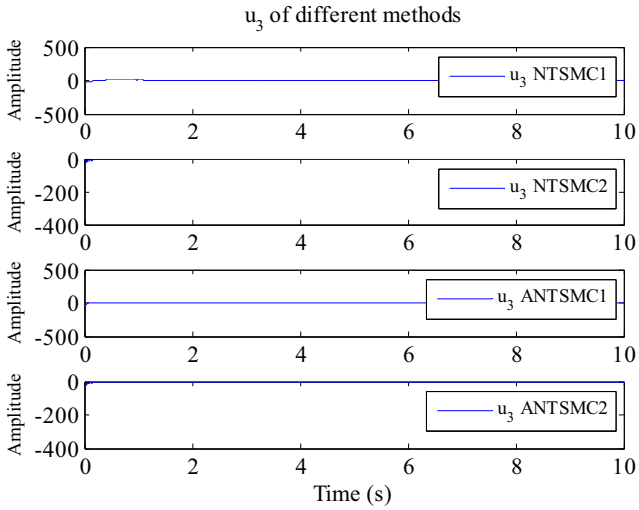

Fig. 11 The control inputs $\boldsymbol{u_3}$ of four proposed control methods

To reveal the effectiveness of the designed controllers in this study, we have performed the numerical simulation by using the control input of FOASMC which has been presented in [14] for the considered smart grid chaotic system in Eq. (3). In fact, the numerical simulation of FOASMC has been done to calculate the numerical value of the performance criteria and to make a comparison with our proposed control methods. The considered control parameters for the numerical simulations of the FOASMC has been presented in [14]. Note that the exact same initial conditions have been considered for all numerical simulations in this study which have been presented in [14] and Sections "3 and 5" of this article.

The value of the performance criteria is calculated by using the Trapezoidal method, implemented in the software Matlab® through command "***trapz*(*t*, *Xi*)**" and the numerical results are presented in Table 2.

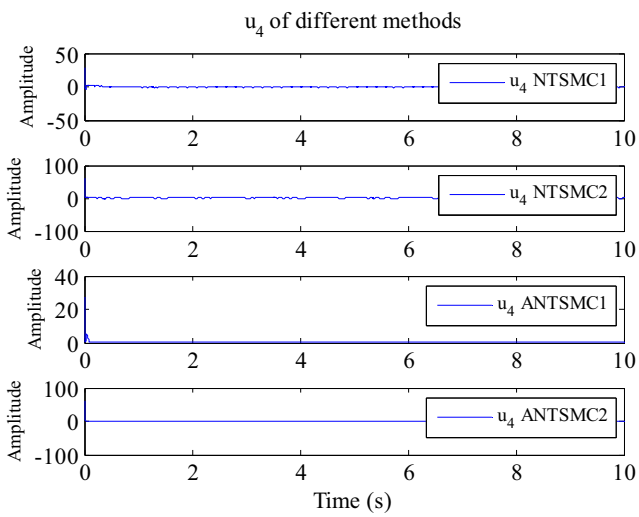

Fig. 12 The control inputs $\boldsymbol{u_4}$ of four proposed control methods

Table 2 Performance criteria for different methods

	NTSMC1	NTSMC2	ANTSM1	ANTSM2	FOASMC
IAE1	0.1142	0.2717	0.0056	0.1332	0.0242
IAE2	0.0119	0.2427	0.0032	0.1042	0.0152
IAE3	0.0057	0.2072	0.0012	0.0685	0.0067
IAE4	0.0679	0.4098	0.0288	0.2705	0.0877
ITAE1	0.9792	0.5115	0.0021	0.0142	0.2761
ITAE2	0.0930	0.5102	0.0017	0.0128	0.1716
ITAE3	0.0858	0.5084	0.0014	0.0107	0.0736
ITAE4	0.2904	0.5160	0.0079	0.0189	1.0290
ISV1	46.5377	13.6650	22.2144	14.5287	16.7790
ISV2	90.6944	18.1175	24.7743	16.9378	22.8813
ISV3	5843.8	3949.6	4631.2	3872.5	4622.5
ISV4	84.8396	154.8209	36.1542	159.3897	68.5617

Figures 13, 14, and 15 represent the mean of each performance criterion for different considered control methods in the comparison section.

The key points of the comparison are listed as follows,

- As shown in Fig. 15, both proposed adaptive control methods (ANTSMC1 and ANTSMC2) and the proposed NTSMC2 method have a smaller value for the ISV than two other methods. Note that, The ISV criterion is related to the amplitude of the control input and lower values of ISV can be deduced as the lower cost of construction and lower consumption of energy. Accordingly, ANTSMC1, ANTSMC2, and NTSMC2 methods are more cost-effective than two other methods in terms of constructing control inputs.
- In terms of the value of ITAE criterion, both proposed adaptive control methods (ANTSMC1 and ANTSMC2) and the proposed NTSMC1 method are more appropriate (due to a smaller value of ITAE) than two other methods.

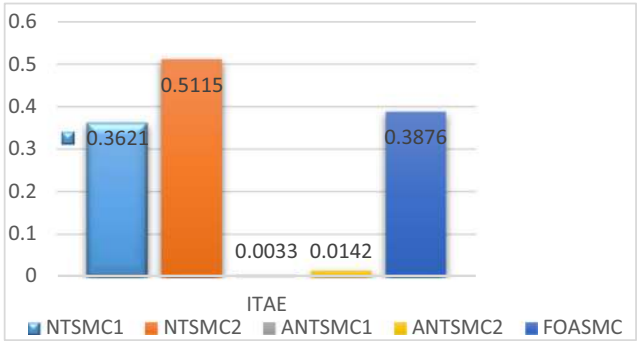

Fig. 14 Comparison of the mean of different methods in terms of the ITAE criterion

- In terms of the value of the IAE criterion, the proposed ANTSMC1 method provides the best controller for the smart grid chaotic system (due to a smaller value).
- The NTSMC1 method in its control input creates the chattering problem as it is predicted (see Figs. 9 to 12). However, this destructive phenomenon is eliminated thoroughly in the proposed NTSMC2, ANTSMC1, and ANTSMC2 methods.
- In terms of constructing control inputs, the NTSMC1 and ANTSMC1 methods (where at their sliding surfaces the integral elements are used) in comparison to the other two methods, NTSMC2 and ANTSMC2 (where at their sliding surfaces the derivative elements are used) are superior. Note that the derivative elements not only boosts the noise, but it is also difficult to construct an ideal derivative element.

Conclusion

In this paper, two robust finite time controllers are designed to synchronize dual smart grid chaotic systems by using non-

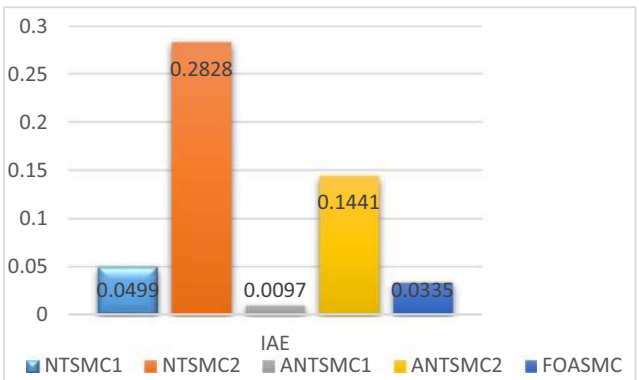

Fig. 13 Comparison of the mean of different methods in terms of the IAE criterion

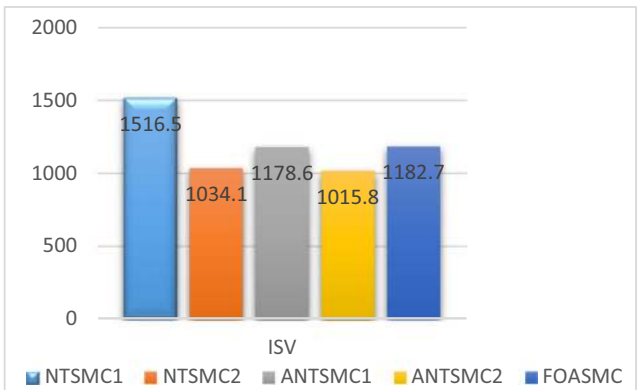

Fig. 15 Comparison of the mean of different methods in terms of the ISV criterion

adaptive and adaptive control methods based-on NTSMC. The adaptive and non-adaptive controllers based on NTSMC are proposed to provide two alternatives which can adjust by changing operating conditions and dynamics as well as comparing them. The numerical simulation results are carried out to show the validity of the four proposed controllers for synchronization objective. Then, by performing the simulation for the FOASMC controller and using three performance criteria, a comprehensive comparison is made among the proposed controllers in this study and FOASMC controller. In terms of the numerical values of the performance criteria, our proposed control methods (especially the proposed adaptive control methods) outperform FOASMC method. The key features of the proposed control methods in this study are finite time stability and robustness against a variety of uncertainties and external disturbances. The elimination of undesirable chattering problem is also addressed in this study. Additionally, the upper bounds of uncertainties and external disturbances are estimated in a finite time in the proposed adaptive control methods.

References

1. Abadi ASS, Hosseinabadi PA (2018) Fuzzy adaptive finite time control ship fin stabilizing systems model of fuzzy Takagi-Sugeno with unknowns and disturbances. Paper presented at the Fuzzy and Intelligent Systems (CFIS), 2018 6th Iranian Joint Congress on
2. Abadi ASS, Hosseinabadi PA, Mekhilef S (2017) Two novel AOTSMC of Photovoltaic system using VSC model in smart grid. Paper presented at the Smart Grid Conference (SGC), 2017
3. Aimad A, Madjid K, Mekhilef S (2014) Robust sensorless sliding mode flux observer for DTC-SVM-based drive with inverter nonlinearity compensation. Journal of Power Electronics 14(1):125–134
4. Al-Dabbagh RD, Kinsheel A, Mekhilef S, Baba MS, Shamshirband S (2014) System identification and control of robot manipulator based on fuzzy adaptive differential evolution algorithm. Adv Eng Softw 78:60–66
5. Bhat SP, Bernstein DS (1998) Continuous finite-time stabilization of the translational and rotational double integrators. IEEE Trans Autom Control 43(5):678–682
6. Carlini E, Giannuzzi G, Mercogliano P, Schiano P, Vaccaro A, Villacci D (2016) A decentralized and proactive architecture based on the cyber physical system paradigm for smart transmission grids modelling, monitoring and control. Technology and Economics of Smart Grids and Sustainable Energy 1(1):5
7. Chu C-C, Iu HH-C (2017) Complex Networks Theory For Modern Smart Grid Applications: A Survey. IEEE Journal on Emerging and Selected Topics in Circuits and Systems
8. Elsayed BA, Hassan M, Mekhilef S (2013) Decoupled third-order fuzzy sliding model control for cart-inverted pendulum system. Appl Math 7(1):193–201
9. Elsayed BA, Hassan MA, Mekhilef S (2015) Fuzzy swinging-up with sliding mode control for third order cart-inverted pendulum system. International Journal of Control. Automation, and Systems 13(1):238
10. Elshaafi H, Vinyals M, Grimaldi I, Davy S (2018) Secure Automated Home Energy Management in Multi-Agent Smart Grid Architecture. Technology and Economics of Smart Grids and Sustainable Energy 3(1):4
11. Fan X, Zhang X, Wu L, Shi M (2017) Finite-time stability analysis of reaction-diffusion genetic regulatory networks with time-varying delays. IEEE/ACM transactions on computational biology and bioinformatics 14(4):868–879
12. Hu J, Pota HR, Guo S (2014) Taxonomy of Attacks for Agent-Based Smart Grids. IEEE Trans Parallel Distrib Syst 25(7):1886–1895
13. Karami-Mollaee A, Tirandaz H, Barambones O (2018) On dynamic sliding mode control of nonlinear fractional-order systems using sliding observer. Nonlinear Dynamics, 1–15
14. Karthikeyan A, Rajagopal K (2017) Chaos control in fractional order smart grid with adaptive sliding mode control and genetically optimized PID control and its FPGA implementation. Complexity, 2017
15. Khazaei J, Nguyen DH (2017). Multi-Agent Consensus Design for Heterogeneous Energy Storage Devices with Droop Control in Smart Grids. IEEE Transactions on Smart Grid
16. Khooban MH, Niknam T, Blaabjerg F, Dehghani M (2016) Free chattering hybrid sliding mode control for a class of non-linear systems: electric vehicles as a case study. IET Sci Meas Technol 10(7):776–785
17. Law YW, Pota HR, Jin J, Man Z, Palaniswami M (2014) Control and communication techniques for the smart grid: An energy efficiency perspective. IFAC Proceedings Volumes 47(3):987–998
18. Li X, Mao W (2016) Finite-time stability and stabilisation of distributed parameter systems. IET Control Theory & Applications 11(5):640–646
19. Liu H, Zhang T (2014) Adaptive neural network finite-time control for uncertain robotic manipulators. J Intell Robot Syst 75(3–4): 363–377
20. Parsegov S, Polyakov A, Shcherbakov P (2013) Fixed-time consensus algorithm for multi-agent systems with integrator dynamics. Paper presented at the 4th IFAC workshop on distributed estimation and control in networked systems
21. Pattabiraman D, Lasseter R, Jahns T (2017) Feeder flow control method with improved power sharing performance in microgrids. Paper presented at the Power & Energy Society General Meeting, 2017 IEEE
22. Pilloni A, Pisano A, Usai E (2018) Robust finite-time frequency and voltage restoration of inverter-based microgrids via sliding-mode cooperative control. IEEE Trans Ind Electron 65(1):907–917
23. Qiao L, Zhang W (2017) Adaptive non-singular integral terminal sliding mode tracking control for autonomous underwater vehicles. IET Control Theory & Applications 11(8):1293–1306
24. Rahman M, Mahmud M, Pota H, Hossain M (2015) A multi-agent approach for enhancing transient stability of smart grids. Int J Electr Power Energy Syst 67:488–500
25. Sajadi A, Sebtahmadi SS, Koniaka M, Biczel P, Mekhilef S (2012) Distributed control scheme for voltage regulation in smart grids. International Journal of Smart Grid and Clean Energy
26. Shi Y, Tuan HD, Savkin A, Duong TQ, Poor HV (2018) Model predictive control for smart grids with multiple electric-vehicle charging stations. IEEE Transactions on Smart Grid
27. Su X, Liu X, Shi P, Yang R (2017) Sliding mode control of discrete-time switched systems with repeated scalar nonlinearities. IEEE Trans Autom Control 62(9):4604–4610
28. Sun Q, Wang Y, Yang J, Qiu Y, Zhang H (2014) Chaotic dynamics in smart grid and suppression scheme via generalized fuzzy hyperbolic model. Mathematical Problems in Engineering, 2014
29. Torres FJ, Guerrero GV, Garcia CD, Gomez JF, Adam M, Escobar RF (2016) Master-slave synchronization of robot manipulators driven by induction motors. IEEE Lat Am Trans 14(9):3986–3991

30. Uddin F (2017) Energy-Aware Optimal Data Aggregation in Smart Grid Wireless Communication Networks. IEEE Transactions on Green Communications and Networking 1(3):358–371
31. Wang H, Man Z, Kong H, Zhao Y, Yu M, Cao Z et al (2016) Design and Implementation of Adaptive Terminal Sliding-Mode Control on a Steer-by-Wire Equipped Road Vehicle. IEEE Trans Ind Electron 63(9):5774–5785
32. Wang X, Yaz EE (2016) Smart power grid synchronization with fault tolerant nonlinear estimation. IEEE Trans Power Syst 31(6): 4806–4816
33. Wu Z-G, Shi P, Su H, Chu J (2014) Local synchronization of chaotic neural networks with sampled-data and saturating actuators. IEEE transactions on cybernetics 44(12):2635–2645
34. Wu Y, Wei Z, Weng J, Li X, Deng RH (2018) Resonance attacks on load frequency control of smart grids. IEEE Transactions on Smart Grid 9(5):4490–4502
35. Xiaohui X, Lining S, Zhijiang D, Hegao C (2005) Internet-based event synchronization communication driven telerobotics. J Syst Eng Electron 16(2):341–345
36. Xu Q (2017) Precision Motion Control of Piezoelectric Nanopositioning Stage With Chattering-Free Adaptive Sliding Mode Control. IEEE Trans Autom Sci Eng 14(1):238–248
37. Zong G, Ren H, Hou L (2016) Finite-time stability of interconnected impulsive switched systems. IET Control Theory & Applications 10(6):648–654